On the Modeling of Polycrystalline Ferroelectric Thin Films: Landau-Based Models Versus Monte Carlo-Based Models Versus Experiment

Mischa Thesberg[ID], Md Nur K. Alam[ID], Brecht Truijen[ID], *Associate Member, IEEE*, Ben Kaczer,
Philippe J. Roussel[ID], Zlatan Stanojević[ID], *Senior Member, IEEE*, Oskar Baumgartner[ID], *Member, IEEE*,
Franz Schanovsky[ID], Markus Karner, *Member, IEEE*, and Hans Kosina, *Member, IEEE*

Abstract—Due to the potential for technological application, there has been an explosion of interest in heavily polycrystalline ferroelectric nanofilms, such as those of doped hafnium oxide. However, the heavily polycrystalline nature of these materials invalidates conventional modeling approaches as the dynamics have been found to be: 1) nucleation-limited; 2) involve grains of ferroelectric material interspersed among grains of alternative, nonferroelectric material; and 3) the direct interaction between these grains is observed to be minimal. In this article, we consider seven separate compact or "0-D" models of such polycrystalline films. Four of these models are based on a Landau paradigm and two are based on a Monte Carlo (MC) paradigm. The seventh is the traditional Preisach model. Although all of these models have been used in the literature to model novel polycrystalline ferroelectric nanofilms, here we compare and contrast the accuracy and physical appropriateness of each model by comparing both their static and dynamic properties against experimental data. We then find that although all models except single-grain models are capable of reproducing the static properties, only the MC models replicate the long-time dynamical properties. Thus, it is demonstrated that not all models are equally valid for the accurate modeling of such films.

Index Terms—Ferroelectric devices, ferroelectric films, Monte Carlo (MC) methods, semiconductor device modeling.

I. INTRODUCTION

ALTHOUGH the study of ferroelectrics has a long history in physics—summarized, for example, in [3]–[5]—in recent years, there has been an explosion of renewed interest in such materials prompted by the discovery of ferroelectricity in the hafnium oxide material system [6]–[8]. The reason for this is twofold. First, hafnium oxide is instantly compatible with preexisting manufacturing flows for integrated circuits since it is already in use as the gate oxide of commercial field-effect transistors. Second, hafnium oxide thin films maintain their ferroelectricity even when thinned to the nanometer scale, making them potentially possible for hafnium-based ferroelectric devices to be competitive with conventional, nano-sized devices. In fact, hafnium oxide only *becomes* ferroelectric below a certain critical thickness. Both these properties are in contrast to "traditional" ferroelectric materials [9] such as lead zirconate titanate (i.e., PZT) and barium titanate (BTO), which lose their ferroelectricity in nanometer-thin films and have faced difficulty with integration into existing manufacturing flows for digital circuits.

The focus of this revitalized activity has largely centered on three classes of device application, which, in order of increasing ambition, are: 1) a conventional memory within a capacitor structure [i.e., ferroelectric random-access memory (FRAM or FeRAM)], which involves a so-called metal–ferroelectric–metal (MFM) structure; 2) a device which combines the functions of both memory and logic in a single structure [i.e., ferroelectric field-effect transistors (FeFETs)] [10], [11] and involves either a metal–ferroelectric–insulator–semiconductor (MFIS) or an MFM–insulator–semiconductor (MFMIS) structure; or 3) a novel type of device, which exploits the somewhat controversial (see, e.g., [12]–[19]) "negative capacitance" effect to produce enhanced performance beyond the theoretical "Boltzmann" limit of conventional field-effect transistors (i.e., NCFETs). This "negative capacitance" effect [20] is most ably described by Landau phase-transition theory [21] for a single-crystalline grain and thus this model sees much use in the literature despite the hafnium oxide-based films being demonstrably heavily polycrystalline [22]–[25] with ferroelectric grains being embedded among a mixture of grains exhibiting other nonferroelectric metallurgical phases.

TABLE I
CATEGORIZATION OF MODELS

	Landau-based	MC-based
Static	Single Grain Landau-Devonshire (SGLD)	Monte Carlo Preisach (MCP)
	Multi-Grain Landau-Devonshire (MGLD)	
Dynamic	Single Grain Landau-Khalatnikov (SGLK)	Monte Carlo Nucleation-Limited-Switching (MCNLS)
	Multi-Grain Landau-Khalatnikov (MGLK)	Thermally-Assisted Nucleation-Limited-Switching (TANLS)

Furthermore, in addition to these three main types of devices, there have also been a number of other novel proposed applications for these ferroelectric films [26]–[28].

The goal of this article is then to take experimental data, chosen to give a kind of representative cross section of both the static and dynamic properties of a ferroelectric hafnium-based film and seven distinct models of ferroelectricity, including single-grained Landau theory, and compare and contrast the physical appropriateness of each model as a descriptor of real devices. More specifically, the models considered here can all be described as *compact* or "0-D" in that they encapsulate the entire ferroelectric response into a single polarization variable. There exist a number of other models in the literature [29]–[32], which consider polarization response in the context of a full 2-D or 3-D system. It is not the goal of this article to consider such models. Rather, the aim is to consider, if one takes a completely agnostic stance on the implications of a given ferroelectric model, which model actually fits experimental data the best.

II. MODELS

In order to focus solely on the ferroelectric material properties without the confounding influence of charge trapping and the distinction between MFM–insulator–metal (MFMIM) structures and metal–ferroelectric–insulator–metal (MFIM) structures, the discussion here will be limited to the consideration of ferroelectric capacitors, that is, MFM structures.

A. Landau-Based Models (SGLD, SGLK, MGLD, and MGLK)

In Landau-based models, the ferroelectric film is considered to be comprised of a number of grains. In this work, we consider the possibility of both single-grain (SG) and multigrain (MG) compact or "0-D" models. The distinction that these models are compact is an important one as there is a wider range of Landau-based models, which considered spatial effects such as gradient terms, that are not considered here. We further consider two classes of Landau models: Landau–Devonshire (LD), which has no time dependence, and Landau–Khalatnikov, which is governed by a dynamical equation with explicit time dependence. In the MG Landau–Devonshire (MGLD) model, the polarization, P_i, of a grain i at a given moment is determined by solving the algebraic equation

$$(E - E_{i,i}) = 2\alpha_i P_i + 4\beta_i P_i^3 \quad \text{(MGLD)} \quad (1)$$

which represents the minimization of a prototypical double-well Landau free energy [21] associated with an ordered phase such as ferroelectricity. E represents the average electric field within the ferroelectric film, or more accurately the projection of the electric field along the polarization axis though all models here are assumed uniaxial, and $E_{i,i}$ represents an intrinsic field E_i of the ith grain and bundles together any complex microscopic detail of the grain's surrounding physical environment into an effective emergent biasing field. The coefficients α_i and β_i are also assumed to vary from grain to grain. However, to aid conceptual clarity and ease comparison between models, these coefficients can be recast as a *coercive field* and a *remnant polarization* according to

$$E_{c,i} = \frac{4|\alpha_i|}{3\sqrt{3}}\sqrt{\frac{|\alpha_i|}{2\beta_i}}, \quad P_{r,i} = \sqrt{\frac{|\alpha_i|}{2\beta_i}} \quad (2)$$

with the total polarization of the film then being the average of the polarization state of the grains, $P_{\text{tot}} = \sum_{i=1}^{n_g} P_i/n_g$, where n_g is the number of grains.

Thus, an MGLD model is then defined by generating a statistical ensemble of grains, each with their own E_i, E_c, and P_r. In this work, it was found that a simple Gaussian distribution for E_i and E_c was sufficient to match experimental data. Thus, the key parameters are P_r, which is assumed the same for each grain, as well as the means and standard deviations of the two fields: $\langle E_i \rangle$, σ_{E_i}, $\langle E_c \rangle$, and σ_{E_c}. The SG Landau–Devonshire (SGLD) model is simply the limiting case of MGLD with only one grain and $E_c = \langle E_c \rangle$ and $E_i = \langle E_i \rangle$.

One could argue that P_r should also be statistically distributed or that there is no particular justification for a Gaussian distribution over any other, such as a Lorentzian or log-normal distribution. Furthermore, experiments have shown (see, e.g., [33] and [1]) that for a non-"woken-up" hafnium zirconium oxide (HZO) film that the distribution of intrinsic fields is actually of two Gaussians, symmetrically placed about the $E_i = 0$ line in the (E_c, E_i)-plane that only migrate and coalesce in field space to a single Gaussian at $E_i = 0$ after cycling. These points are valid and the only justification given here for this choice is that it is sufficient to achieve an excellent match to experimental data, as will be seen in Sections III and IV.

The MG Landau–Khalatnikov (MGLK) model promotes the MGLD model into a dynamic differential equation

$$\frac{dP_i}{dt} = \rho_i \big(2\alpha_i P_i + 4\beta_i P_i^3 - (E - E_{i,i})\big) \quad \text{(MGLK)} \quad (3)$$

where switching then exhibits a characteristic switching time related to the parameter $1/\rho_i$ which may also statistically vary from grain to grain. However, for this work, it was found that a uniform ρ for all grains was sufficient to match experiment provided α_i and β_i (or E_c and E_i) have a statistical spread.

Finally, it is worth reiterating that although these MGLD and MGLK include multiple grains, there is no explicit coupling

between grains as might be found in a 2-D or 3-D Landau model involving gradient and grain-boundary energy terms. Such more complex models are not under consideration here, although it must be said that any claims made with respect to the utility of the compact MGLD and MGLK models considered here, cannot be said to also apply to those more complex phase-field-type models.

B. Monte Carlo (MC) Models (MCP, MCNLS, and TANLS)

The following models can all be qualified as being of the Monte Carlo (MC) type. In all such models, the simulation is divided into discrete time steps with a certain applied field associated with that time step. The ferroelectric response is then determined by considering a discrete ensemble of switching units that can switch between a +1 and −1 state according to a certain field-dependent probability. The functional behavior of this probability depends on the specific model and its specific physical assumption. Random numbers are then generated for each switching unit and for those where the random number is below the switching probability, their switching state is flipped. The total polarization is then the average of all switching units.

1) MC Preisach Model: The well-known Preisach model [34] seeks to model hysteretic systems by describing their behavior in terms of an ensemble of abstractified fundamental switching units called *hysterons*. Each hysteron can hold only one of two binary states, $P_i = \pm 1$, and the total polarization is then the average state of these hysterons weighted by a single total remnant polarization of the system: $P_{\text{tot}} = P_r \sum_i^{n_g} P_i / n_g$. Although each hysteron is assumed to equally contribute to the total polarization, a choice justified by match to experiment, each has its own "flip up" field, $E_\uparrow$, and "flip down" field, $E_\downarrow$, such that a hysteron in the state $P_i = -1$ will remain there until it experiences a field $E - E_i > E_\uparrow$ at which point it will transition to the $P_i = +1$. The opposite meaning then applies for the field $E_\downarrow$.

As before, for ease of conceptual interpretation, rather than speaking in terms of $E_\uparrow$ and $E_\downarrow$ fields, it is beneficial to recast them in terms of *coercive fields*, E_c, and *intrinsic fields*, E_i, according to the definitions

$$E_c = \frac{E_\uparrow - E_\downarrow}{2}, \quad E_i = \frac{E_\uparrow + E_\downarrow}{2}. \quad (4)$$

In the traditional Preisach model, there are assumed to be an infinite number of hysterons defined by a continuous distribution $f(E_\downarrow, E_\uparrow)$ (or $f(E_c, E_i)$) such that $f(E_\downarrow, E_\uparrow)dE_\downarrow dE_\uparrow$ represents the fraction of hysterons with flip up/down fields in the interval $[E_\downarrow, E_\downarrow + dE_\downarrow] \times [E_\uparrow, E_\uparrow + dE_\uparrow]$. However, here, we assume an *MC* implementation where a finite number of hysterons are considered with fields drawn from the Gaussian distributions defined by $\langle E_i \rangle$, σ_{E_i}, $\langle E_c \rangle$, and σ_{E_c}. In the limit of infinitely many hysterons, the two descriptions are numerically equivalent.

2) MC Nucleation-Limited-Switching Model: The Preisach model is well suited to the description of the major and minor hysteretic loops of a ferroelectric. However, it is fundamentally a *static* model with its hysterons responding instantaneously to a given applied field. Thus, it is incapable of modeling any form of transient ferroelectric behavior. To capture such dynamical behavior, we considered two additional models, the first of which is the MC nucleation-limited-switching (MCNLS) model.

The MCNLS model is conceptually very similar to an MC-based Preisach model except instead of having clear abrupt flip up/down fields above/below which switching is guaranteed and below/above switching never occurs, hysterons instead have an activation field, E_a, that dictates a characteristic switching time, $\tau_{\text{sw}}(E)$, dependent on the current applied field according to Merz' law [35], a power-law relation

$$\tau_{\text{sw},i}(E)$$
$$= \begin{cases} \tau_0 \exp\left(\left(\frac{E_{a,i}}{|E - E_{i,i}|}\right)^\alpha\right), & \text{sign}(P_i) \neq \text{sign}(E - E_{i,i}) \\ \infty, & \text{otherwise} \end{cases}$$
$$(5)$$

where τ_0 is the *intrinsic switching time*, $E_{i,i}$ is an intrinsic biasing field with the same meaning as previously, and α is a fittable exponent with a typical value of 2–3 (and is unrelated to α_i being the linear coefficient of Landau-based models). It is important to note the piecewise definition with respect to the sign of $E - E_{i,i}$. Thus, "up switching" only occurs when the applied field is greater than E_i and "down switching" only when it is less than E_i.

The instantaneous characteristic switching time, τ_{sw}, then defines a probability per unit time of a given hysteron i with activation field $E_{a,i}$ to flip. In the most general case, this switching probability, p_{sw}, can be considered to be a memory-having Weibull process

$$p_{\text{sw},i} = 1 - \exp\left(-(h_i(t + \Delta t)^n - h_i(t)^n)\right) \quad (6)$$

where $h_i = \int_{t=0}^t dt/\tau_{\text{sw},i}(E(t))$ and n controls the level of Weibull-ness. Although such generalized switching behavior has been considered in the literature [36], [37], here it was found sufficient to assume a simple Poisson process, corresponding to $n = 1$, where switching per unit time has no dependence on any previous time. Though generically one could consider the exponent n as an additional tunable parameter, even if that is not done so here.

Thus, an MCNLS simulation proceeds time-step by time-step, where at each step of Δt, the current field, $E(t)$, determines the switching probability for each hysteron, and whether a given switch occurs is dictated by random number generation. Thus, unlike the Preisach model, a given hysteron can potentially change states at any field (provided $E - E_{i,i}$ has the correct sign) only with exponentially suppressed probability at low fields.

Thus, the key parameters of the MCNLS model are $\langle E_a \rangle$, σ_{E_a}, $\langle E_i \rangle$, σ_{E_i}, α and τ_0 (which is assumed to be the same for all hysterons).

3) Thermally Activated Nucleation-Limited-Switching Model: The final model considered in this work is the thermally activated nucleation-limited-switching (TANLS) model championed in [38]. Conceptually, this model exists as a kind of middle ground between the MGLK and MCNLS models and considers a grain or hysteron (the distinction will be a

matter of discussion shortly) subject to a Landau double-well free energy landscape. However, rather than the polarization state, P_i, being a continuous value obtained from solving algebraic (1) instead P_i is assumed to only take the values ± 1 corresponding to in which of the two wells the system currently resides. Furthermore, transitions from one well to the other are not assumed to occur only when the double-well loses its central maxima (i.e., "rolling downhill") but rather are considered to be a thermally-driven process over a potential barrier.

Thus, TANLS recasts a Landau-based perspective into an MC model parameterized by: 1) the energy barrier W_b which separates the two wells

$$W_{b,i} = \frac{3\sqrt{3}}{8} E_{c,i} P_r \qquad (7)$$

2) a critical volume at which a nucleus of reversed polarization is thermodynamically stable against spontaneous collapse, V_*, which typically has a value of 3–5 nm³; and 3) an *attempt frequency*, ν_0, which is often associated with the available thermal energy for a scattering process (e.g., an optical phonon energy - which are typically in the 20–100 meV range - amounts to an attempt frequency of approximately 10^{13} Hz). The final expression for the characteristic switching time in TANLS as a function of these parameters is then

$$\tau_{sw} = \frac{1}{\nu_0} \exp\left[\frac{V_*}{k_b T} \times \left(W_{b,i} + P_i P_r (E - E_{i,i}) \right) \right]. \qquad (8)$$

For further discussion of this model, see [38]. As with the MCNLS model, this τ_{sw} most generally then feeds into a Weibull process according to (6) but here it was also found that a Poisson process ($n = 1$) was sufficient. Furthermore, the critical nucleus size and attempt frequency were assumed to be material properties of the ferroelectric phase itself and thus do not vary from grain to grain. Thus, as before, the key parameters are the Gaussian-distributed parameters $\langle E_i \rangle$, σ_{E_i}, $\langle E_c \rangle$, and σ_{E_c} as well as P_r, ν_0, and V_*.

C. General Discussion of the Models

The seven models considered in this work can be categorized in two ways: 1) whether they are dynamic or static or 2) whether they are Landau-based or MC-based. The way each model fits into these categorization criteria is detailed in Table I. Static models have a polarization response to a given field that is instantaneous. Conversely, dynamic models have a characteristic time-scale associated with their polarization response that is field-dependent. In the generalized case of a Weibull process, where n in (6) is greater than 1, their response may also be explicitly dependent on the history of the applied field.

With regard to the second criterion of categorization, a Landau-based model is deterministic and its behavior is dictated by solving an algebraic equation where an MC model has stochastic dynamics driven by random-number generation and the random flipping of hysterons. In this work, the classic Preisach model MC Preisach (i.e., MCP) is also conceptualized as a type of MC model even if it has no explicit random number generation in its dynamics as it still

considers an ensemble of discrete switching hysterons. The TANLS model is also of special note because, although its physical motivation is based on Landau's free energy-based reasoning, it is ultimately an MC model. Furthermore, it is unique among the seven in that it has explicit temperature dependence (note that although Landau models often have a temperature dependence associated with the linear term of (1) and (3), $\alpha_i = -|\alpha_0|(T - T_c)$, this dependence controls the existence of the ferroelectric ordered phase itself, not the speed of the switching dynamics). However, the physical accuracy of its temperature dependence in replicating the true thermal behavior of polycrystalline films will not be considered here.

Furthermore, there is some debate as to whether the "grains" of multigrained models are truly connected to physical metallurgical grains or are best also interpreted as an abstracted entity like "hysterons." Here, we maintain the common practice of the literature in referring to Landau "grains" without specifically claiming that these should be interpreted as such. Furthermore, as has previously been discussed, although there exist a larger class of Landau models that considered spatiality and explicit gradient and grain–grain interaction terms, these are not what is under consideration in this work. Thus, the "grains" considered here are directly constructed as uncoupled and independently switching, which further softens any conceptual connection to real, physical metallurgical grains within the film.

The final key distinction between the models that warrants discussion is their treatment of the much-debated [12]–[16] (quasi-static) "negative capacitance" effect in ferroelectric layered structures, such as MFIM or MFIS structures. Although this work focuses on the response within a capacitor (i.e., an MFM) structure this question deserves some consideration. However, as has been shown in the literature, any dynamical model, including the MC models considered here, can replicate "negative capacitance" via transient effects driven by a resistive delay in switching (see [15] or [16]) or as simply "reverse switching" (see [39]). Furthermore, the paradigmatic quasi-static "negative capacitance" scenario involves traversing the so-called "S-curve" of a Landau-based model. Such a thing becomes impossible in multigrained Landau models with a sufficient spread in their intrinsic and coercive fields. Thus, all models considered here agree with a transient explanation of observed "negative capacitance" and the only models considered here [SGLD and single-grain Landau–Khalatnakov (SGLK)] that fit with the more attractive quasi-static "S-curve"-based "negative capacitance" will be found to be poor models of experimental data.

III. MODELS VERSUS FORC MEASUREMENTS

In this work, the seven ferroelectric models are pitted against two separate types of experimental measurements. The first of these is a first-order reversal curve (FORC) measurement on a ferroelectric capacitor and is intended to validate the ability of the models to reproduce the *static* characteristics of a polycrystalline ferroelectric film. What is meant by "static properties" is that a FORC measurement involves a relatively slowly applied wavepulse and thus the observed ferroelectric response is expected to be solely due to the landscape of

TABLE II
BEST-FIT PARAMETERS: FORC

	P_r [μC/cm^2]	$\langle E_c \rangle$ [MV/cm]	σ_{E_c} [MV/cm]	$\langle E_i \rangle$ [MV/cm]	σ_{E_i} [MV/cm]	Other	SSD
SGLD	9.07	1.22	-	0.0	-	-	11.0×10^{-4}
SGLK	0.513	2347	-	0.282	-	$\rho = 0.111$ m$\Omega \cdot m$	6.56×10^{-4}
SGLK	0.00487	2.78×10^{-5}	-	0.0	-	$\rho = 8.95 \times 10^{-2}$ m$\Omega \cdot m$	8.59×10^{-4}
MGLD	14.5	1.14	0.135	0.260	0.644	-	2.23×10^{-4}
MGLD	14.5	1.47	0.847	0.0	0.0	-	1.27×10^{-4}
MGLK	14.8	1.21	0.348	0.305	0.686	$\rho = 90.3$ m$\Omega \cdot m$	0.945×10^{-4}
MGLK	13.6	1.37	0.840	0.0	0.0	$\rho = 22.1$ m$\Omega \cdot m$	1.39×10^{-4}
MCP	15.1	1.28	0.764	0.0	0.0	-	1.92×10^{-4}
MCNLS	14.0	2.03 (E_a)	1.38 (E_a)	0.0	0.0	$\alpha = 2.24$, $\tau_0 = 127$ ns	1.24×10^{-4}
TANLS	14.3	3.88	1.14	0.0	0.0	$h\nu_0 = 345$ meV, $V_\star = 4.47$ nm^3	1.14×10^{-4}

coercive and intrinsic fields of the grains or hysterons of the system. In other words, a FORC measurement explores the distribution $f(E_c, E_i)$ as discussed in Section II-B.1.

However, although a FORC measurement is considered a static measurement, it is worth noting that from the perspective of the MCNLS and TANLS MC models, no measurement can truly be fully static. In the MCNLS model, the central object is the field-dependent characteristic switching time and although this switching time becomes exponentially longer, the further E is from the activation field, E_a, it is not infinitely long, and thus given infinite time all hysterons will eventually switch (provided $E > E_i$) at any arbitrarily low field in the MCNLS model. In the TANLS model, both transitions from one free energy potential well to the other *and* from that well back to the original are processes that occur with a certain finite probability in all fields. Thus, for example, when the applied field is removed (i.e., E is returned to zero) if a TANLS film is truly given infinite time, then its hysterons will spend equal time in each well, since their energies are degenerate, resulting in an average polarization of zero and no hysteresis at all. Thus, with regard to the MC models, the term "static" is to be interpreted in a pragmatic sense as meaning "on the order of seconds" or "orders of magnitude slower than the characteristic switching time of most hysterons."

A FORC measurement consists of initially poling a ferroelectric capacitor to the negative polarized state via a large negative voltage and then applying a sequence of triangular pulses of ever-increasing maximum amplitude to the film always returning to the negative poled state at the end of each pulse. In this way, the set of all minor loops originating from the negative poled states and the major loop of the hysteresis are unlocked. The FORC data used in this work were taken from [40] and [41] and were performed on a TiN/ferroelectric Hf$_{0.5}$Zr$_{0.5}$O$_2$/heavily doped Si capacitor with an HZO thickness of 10 nm and an area of 100 μm $\times$ 100 μm. The experimental data exhibited a very strong linear dielectric response including both intrinsic contributions from nonferroelectric grains as well as from the measurement equipment. To focus on only the ferroelectric behavior, this linear contribution to the capacitor charge was subtracted. This was done by simply determining the linear contribution that most resulted in a flat slope at the ends of the major loop.

The original data included ~100 triangular pulses. However, for ease of exposition and clarity, five representative pulses
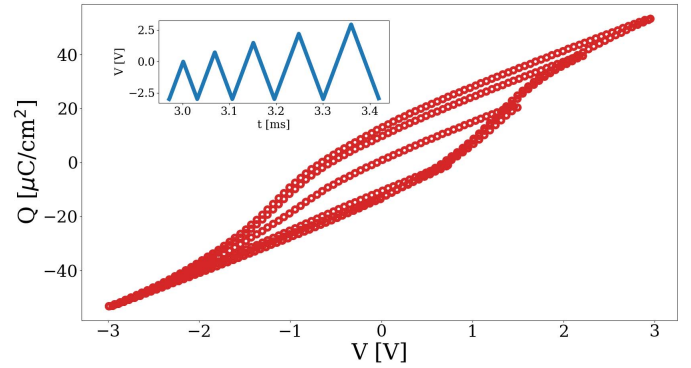

Fig. 1. Five representative pulses extracted from the experimental FORC data of [40] and [41]. Inset: the representative applied waveform.

were extracted from the full set and used for both fitting and plotting. This synthesized pulse, before the aforementioned linear component has been subtracted, can be seen in the inset of Fig. 1. Using this data, each model was subjected to a least-squares statistical fitting model based on Nelders–Mead optimization with the best-fitting parameter values found in Table II. Although any MC simulation involves some random variation from simulation to simulation, even given identical parameters, in the best-fit searching, sample-to-sample variation was found to be insignificant, for the large number of hysterons used, relative to those caused by parameter changes. The final value of the sum-of-squared difference (SSD) of the best fit for each model is also given, for reference. However, as it is not possible to guarantee that the best fit of an optimization algorithm with nonbounded parameters is truly the global minima, these values should not be considered infallible.

The results for the Landau- and MC-based models versus the experimental FORC results are plotted in Fig. 2. As can be seen, all models are capable of producing excellent matches to the measured data except the single-grained ones. It is interesting that the SGLK does have *some* ability to follow the FORC curve but this is misleading as this requires highly unphysical parameters that are likely extremely "hard-coded" to the specific pulse sequence. In other words, the best-fit SGLK has found a time response that is just perfectly right, given the time-scale of the FORC data, to dynamically follow the triangular pulses to "fake" the curve. As a result, the SGLD and SGLK results have highly unphysical parameters.

TABLE III
BEST-FIT PARAMETERS: POLARIZATION CHANGE VERSUS TIME

|	P_r [μC/cm^2]	$\langle E_c \rangle$ [MV/cm]	σ_{E_c} [MV/cm]	$\langle E_i \rangle$ [MV/cm]	σ_{E_i} [MV/cm]	R [μΩ]	C [F]	Other	SSD
SGLD	8.95	0.971	-	0.6389	-	1.35	0.768	-	11.3
SGLD	8.70	0.0430	-	0.0	-	2.02	0.0107	-	53.8
SGLK	0.749	1546	-	0.128	-	0.0	0.0996	$\rho = 0.863\ \Omega \cdot m$	84.0
SGLK	0.00674	1.35×10^{-5}	-	0.0	-	787	0.0900	$\rho = 0.786\ \mathrm{m}\Omega \cdot m$	42.8
MGLD	18.4	0.316	0.0	0.213	0.512	1.4	0.347		11.0
MGLD	19.5	0.596	0.239	0.0	0.0	1.91	0.428		6.76
MGLK	13.4	0.809	0.279	0.0	0.0	0.979	0.218	$\rho = 5.18\ \mathrm{m}\Omega \cdot m$	11.7
MCP	15.8	0.728	0.308	0.0	0.0	1.07	0.773	-	7.06
MCNLS	16.8	1.40 (E_a)	0.609 (E_a)	0.0	0.0	0.935	0.322	$\alpha = 2.60,\ \tau_0 = 49.0$ ns	1.64
TANLS	16.5	2.92	0.562	0.0	0.0	1.09	0.361	$\hbar\nu_0 = 49.3$ meV, $V_\star = 4.00$ nm^3	11.6
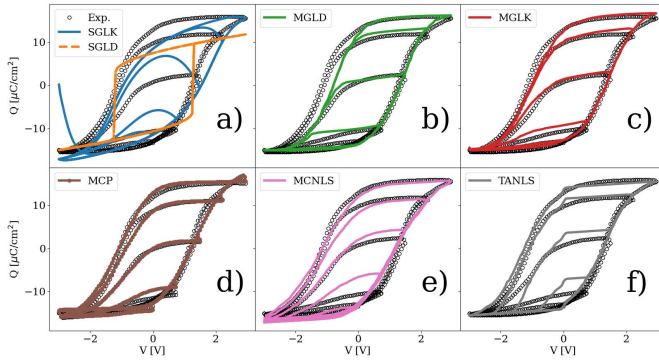
Fig. 2. Polarization versus applied voltage, after the linear charge contribution has been subtracted, for each of the seven ferroelectric models. a) SGLK and SGLD. b) MGLD. c) MGLK. d) MCP. e) MCNLS. f) TANLS.
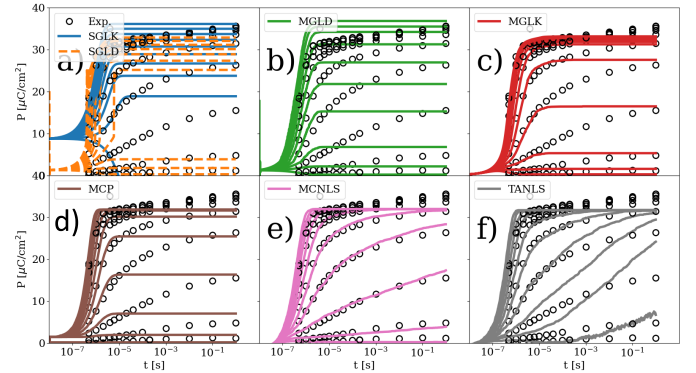

Fig. 3. Change in polarization versus time for an applied step pulse with voltages ranging from 0.25 to 2.25 V for each of the seven ferroelectric models. a) SGLK and SGLD. b) MGLD. c) MGLK. d) MCP. e) MCNLS. f) TANLS.

Additionally, it is interesting to note that a good fit is possible for all models without the need for an experimental spread in intrinsic fields E_i. However, in cases where such a statistical spread leads to some, albeit small, improvement, multiple fits are tabulated; with and without E_i variation.

IV. MODELS VERSUS SWITCHING TIME MEASUREMENTS

Emboldened by the capability of all seven considered models to match the static behavior of a polycrystalline ferroelectric film, it is then worthwhile to consider their validity with respect to their dynamic properties. To do this, we again consider experimental data drawn from [40] and [41] but instead consider the switching time versus applied voltage data. In this measurement, a ferroelectric capacitor of the same size and makeup as that in Section III is initially poled to the negatively saturated polarization state. Then, a single-step pulse is applied of a certain voltage (ranging from 0.25 to 2.25 V) and the resulting change in polarization is tracked as a function of time by integrating the measured capacitive current. Additionally, the linear component of the capacitive charge can be isolated by applying a second pulse after poling, which would exhibit only a linear response, and subtracting off that contribution. Thus, only the true polarization response is plotted.

During that work, it was found that the measured switching speed was ultimately limited by the RC response of the measurement equipment rather than the intrinsic response

of the ferroelectric itself. Thus, the short-time data, on the order of microseconds, are to be considered as a convolution of true ferroelectric dynamics and the measurement circuit response. An important consequence of this is that this data is not to be interpreted as an indication that a ferroelectric film is incapable of switching at submicrosecond speeds since that regime is not accessible via the measurement equipment used. To model this, the ferroelectric models were embedded inside an RC circuit with R and C being fittable parameters.

However, even if the short-time behavior must be considered as a conflation of intrinsic (i.e., the film) and extrinsic (i.e., the measurement circuit) dynamical responses, such data also exhibit noticeable long-time behavior with polarization continuing to rise and exhibit an ongoing response over a time range of at least six orders of magnitude (see also, e.g., [36], [37] for a similar dataset). It is this long-time behavior that is of particular interest as it cannot possibly result from a static model such as the MCP or SGLD/MGLD model whose response is instantaneous. See Fig. 3 for the best attempt to match these models to experimental data. The best-fit fitting parameters for all models can be found in Table III.

However, it is also important to note that the MGLK model seems similarly incapable of reproducing the observed long-time behavior as its dynamical response is linear, parameterized by ρ, and thus it has no mechanism for exhibiting a response over an exponentially wide range of time scales.

One could argue that such behavior might be possible if the underlying distribution of coercive and intrinsic fields [i.e., $f(E_c, E_i)$] was not chosen to have a Gaussian distribution but rather one with a longer exponential tail, such as log-normal. However, it is interesting to note that the MCNLS model shown in Fig. 3 *can* very ably reproduce the observed dynamics over all time scales, better than a "lumped domain" Landau–Khalatnikov (LK)-based approach and thus putting doubt on the physical veracity of such approaches. However, it has been found that more complex 3-D models utilizing an LK-like phase-field model can at least qualitatively reproduce such long-term behavior provided explicitly spatially varying coercive fields are considered [42].

Finally, the results of the TANLS model are shown in Fig. 3. Here, it is seen that although the TANLS model is capable of long-time dynamics, with a polarization response observed even at long time scales, the physical accuracy of this long-time behavior seems to be in poor agreement with the experiment.

Another point of note is that the same parameters for identical devices are found to vary somewhat between Tables II and III. Indeed, attempts (not shown) to simultaneously fit both measurements with a common set of parameters result in markedly poorer fits for all models. It is difficult to confidently indicate the source of these discrepancies but there are likely three possible sources: differing amounts of wakeup, measurement instrumentation differences and overly simplified assumptions of the underlying distributions of key parameters. In both measurements, the devices were precycled. However, for example, the FORC measurement involves over a hundred additional pulses throughout the course of the measurement. It is possible that this produces some further amount of wakeup and thus material parameter variation relative to the other measurement. Another possible origin is the fact that each measurement extracts an estimate of the polarization from a different post-processing approach on a different type of pulse sequence using different measurement devices (for further details, see the original articles [40] and [41]). This may also introduce systematic differences between the two datasets. Yet another contributor is that many quantities are assumed constant or Gaussian that may, if given more complex behavior may allow for a closer match between fitting parameters. However, this would also be at the cost of potentially dramatically increasing the number of unknown variables. Finally, although all models have been described using a set of conceptually similar quantities, such as coercive fields, the actual mathematical role of these same quantities in governing physics is different from model to model. Therefore, one would not expect, for example, E_c to take the same value in two different models, even if it has been given the same name for clarity of concept. Finally, as the models considered here are all "compact" or "0-D," they necessarily must approximate away many microscopic details and encapsulate them in a few rough emergent parameters. Thus, although these models, because of this simplicity and relatively few numbers of parameters, have tremendous utility, some deviation from setting to setting for the same film may be unavoidable.

V. Conclusion

In this work, seven models of polycrystalline ferroelectric thin films were considered: four Landau-based models being the SG, MG, LK, and LD models, two MC-based models being the MC (MCNLS) and thermally assisted (TANLS) nucleation-limited-switching models, and an MC variant of the traditional Preisach (MCP) model were all compared against experimental results on an HZO capacitor. It was found that, despite the broad use of a single-grained Landau model in the literature, such a model is incapable of reproducing either the static or dynamic properties of real HZO films. Furthermore, it was found that Landau models, in general, were poorly able to reproduce the long-time dynamic behavior of such films. Conversely, the MCNLS model was found to give good agreement in all cases.

References

[1] N. Gong, X. Sun, H. Jiang, K. S. Chang-Liao, Q. Xia, and T. P. Ma, "Nucleation limited switching (NLS) model for HfO$_2$-based metal-ferroelectric-metal (MFM) capacitors: Switching kinetics and retention characteristics," *Appl. Phys. Lett.*, vol. 112, no. 26, Jun. 2018, Art. no. 262903.

[2] R. Khachaturyan, J. Wehner, and Y. A. Genenko, "Correlated polarization-switching kinetics in bulk polycrystalline ferroelectrics: A self-consistent mesoscopic switching model," *Phys. Rev. B, Condens. Matter*, vol. 96, no. 5, Aug. 2017, Art. no. 054113.

[3] M. Dawber, K. M. Rabe, and J. F. Scott, "Physics of thin-film ferroelectric oxides," *Rev. Mod. Phys.*, vol. 77, no. 4, p. 1083, 2005.

[4] N. Setter *et al.*, "Ferroelectric thin films: Review of materials, properties, and applications," *J. Appl. Phys.*, vol. 100, no. 5, Sep. 2006, Art. no. 051606.

[5] J. F. Scott, "Applications of modern ferroelectrics," *Science*, vol. 315, no. 5814, pp. 954–959, Feb. 2007.

[6] T. S. Böscke, J. Müller, D. Bräuhaus, U. Schröder, and U. Böttger, "Ferroelectricity in hafnium oxide: CMOS compatible ferroelectric field effect transistors," in *IEDM Tech. Dig.*, Dec. 2011, pp. 24.5.1–24.5.4.

[7] J. Müller *et al.*, "Ferroelectricity in simple binary ZrO$_2$ and HfO$_2$," *Nano Lett.*, vol. 12, no. 8, pp. 4318–4323, 2012.

[8] J. Zhou *et al.*, "Demonstration of ferroelectricity in Al-doped HfO$_2$ with a low thermal budget of 500 °C," *IEEE Electron Device Lett.*, vol. 41, no. 7, pp. 1130–1133, Jul. 2020.

[9] M. Vopsaroiu, J. Blackburn, M. G. Cain, and P. M. Weaver, "Thermally activated switching kinetics in second-order phase transition ferroelectrics," *Phys. Rev. B, Condens. Matter*, vol. 82, no. 2, Jul. 2010, Art. no. 024109.

[10] A. Aziz *et al.*, "Computing with ferroelectric FETs: Devices, models, systems, and applications," in *Proc. Design, Autom. Test Eur. Conf. Exhib. (DATE)*, Mar. 2018, pp. 1289–1298.

[11] J. Hoffman *et al.*, "Ferroelectric field effect transistors for memory applications," *Adv. Mater.*, vol. 22, nos. 26–27, pp. 2957–2961, 2010.

[12] M. A. Alam, M. Si, and P. D. Ye, "A critical review of recent progress on negative capacitance field-effect transistors," *Appl. Phys. Lett.*, vol. 114, no. 9, Mar. 2019, Art. no. 090401.

[13] Z. Liu, M. A. Bhuiyan, and T. P. Ma, "A critical examination of 'quasi-static negative capacitance' (QSNC) theory," in *IEDM Tech. Dig.*, Dec. 2018, pp. 31.2.1–31.2.4.

[14] J. A. Kittl, B. Obradovic, D. Reddy, T. Rakshit, R. M. Hatcher, and M. S. Rodder, "On the validity and applicability of models of negative capacitance and implications for MOS applications," *Appl. Phys. Lett.*, vol. 113, no. 4, 2018, Art. no. 042904.

[15] B. Obradovic, T. Rakshit, R. Hatcher, J. A. Kittl, and M. S. Rodder, "Ferroelectric switching delay as cause of negative capacitance and the implications to NCFETs," in *Proc. IEEE Symp. VLSI Technol.*, Jun. 2018, pp. 51–52.

[16] C. Jin, T. Saraya, T. Hiramoto, and M. Kobayashi, "On the physical mechanism of transient negative capacitance effect in deep subthreshold region," *IEEE J. Electron Devices Soc.*, vol. 7, pp. 368–374, 2019.

[17] S. J. Song *et al.*, "Alternative interpretations for decreasing voltage with increasing charge in ferroelectric capacitors," *Sci. Rep.*, vol. 6, no. 1, pp. 1–6, Feb. 2016.

[18] A. K. Saha, S. Datta, and S. K. Gupta, "'Negative capacitance' in resistor-ferroelectric and ferroelectric-dielectric networks: Apparent or intrinsic?" *J. Appl. Phys.*, vol. 123, no. 10, 2018, Art. no. 105102.

[19] J. Van Houdt and P. Roussel, "Physical model for the steep subthreshold slope in ferroelectric FETs," *IEEE Electron Device Lett.*, vol. 39, no. 6, pp. 877–880, Jun. 2018.

[20] S. Salahuddin and S. Datta, "Use of negative capacitance to provide voltage amplification for low power nanoscale devices," *Nano Lett.*, vol. 8, no. 2, pp. 405–410, 2008.

[21] L. D. Landau and E. M. Lifshitz, *Course of Theoretical Physics: Statistical Physics*, vol. 5. Amsterdam, The Netherlands: Elsevier, 1951.

[22] U. Schroeder *et al.*, "Impact of different dopants on the switching properties of ferroelectric hafniumoxide," *Jpn. J. Appl. Phys.*, vol. 53, no. 8S1, 2014, Art. no. 08LE02.

[23] H. Mulaosmanovic *et al.*, "Switching kinetics in nanoscale hafnium oxide based ferroelectric field-effect transistors," *ACS Appl. Mater. Interfaces*, vol. 9, no. 4, pp. 3792–3798, Feb. 2017.

[24] C. T. Tung, G. Pahwa, S. Salahuddin, and C. Hu, "A compact model of polycrystalline ferroelectric capacitor," *IEEE Trans. Electron Devices*, vol. 68, no. 10, pp. 5311–5314, Oct. 2021.

[25] K. Ni, W. Chakraborty, J. Smith, B. Grisafe, and S. Datta, "Fundamental understanding and control of device-to-device variation in deeply scaled ferroelectric FETs," in *Proc. Symp. VLSI Technol.*, Jun. 2019, pp. T40–T41.

[26] H. Mulaosmanovic, E. T. Breyer, T. Mikolajick, and S. Slesazeck, "Reconfigurable frequency multiplication with a ferroelectric transistor," *Nature Electron.*, vol. 3, no. 7, pp. 391–397, Jul. 2020.

[27] Z. Zhou *et al.*, "A metal-insulator-semiconductor non-volatile programmable capacitor based on a HfAlO$_x$ ferroelectric film," *IEEE Electron Device Lett.*, vol. 41, no. 12, pp. 1837–1840, Dec. 2020.

[28] S. Zheng *et al.*, "Proposal of ferroelectric based electrostatic doping for nanoscale devices," *IEEE Electron Device Lett.*, vol. 42, no. 4, pp. 605–608, Apr. 2021.

[29] H. W. Park, J. Roh, Y. B. Lee, and C. S. Hwang, "Modeling of negative capacitance in ferroelectric thin films," *Adv. Mater.*, vol. 31, no. 32, Jun. 2019, Art. no. 1805266.

[30] A. K. Saha and S. K. Gupta, "Multi-domain negative capacitance effects in metal-ferroelectric-insulator-semiconductor/metal stacks: A phase-field simulation based study," *Sci. Rep.*, vol. 10, no. 1, pp. 1–12, Dec. 2020.

[31] A. K. Saha, M. Si, P. D. Ye, and S. K. Gupta, "Polarization switching in Hf$_{0.5}$Zr$_{0.5}$O$_2$-dielectric stack: The role of dielectric layer thickness," *Appl. Phys. Lett.*, vol. 119, no. 12, Sep. 2021, Art. no. 122903.

[32] A. K. Saha, M. Si, K. Ni, S. Datta, P. D. Ye, and S. K. Gupta, "Ferroelectric thickness dependent domain interactions in FEFETs for memory and logic: A phase-field model based analysis," in *IEDM Tech. Dig.*, Dec. 2020, pp. 4.3.1–4.3.4.

[33] T. Schenk, M. Hoffmann, J. Ocker, M. Pešić, T. Mikolajick, and U. Schroeder, "Complex internal bias fields in ferroelectric hafnium oxide," *ACS Appl. Mater. Interfaces*, vol. 7, no. 36, pp. 20224–20233, Sep. 2015.

[34] F. Preisach, "Über die magnetische nachwirkung," *Zeitschrift Physik*, vol. 94, nos. 5–6, pp. 277–302, 1935.

[35] W. J. Merz, "Domain formation and domain wall motions in ferroelectric BaTiO$_3$ single crystals," *Phys. Rev.*, vol. 95, pp. 690–698, Aug. 1954. [Online]. Available: https://link.aps.org/doi/10.1103/PhysRev.95.690

[36] C. Alessandri, P. Pandey, and A. C. Seabaugh, "Experimentally validated, predictive Monte Carlo modeling of ferroelectric dynamics and variability," in *IEDM Tech. Dig.*, Dec. 2018, pp. 16.2.1–16.2.4.

[37] C. Alessandri, P. Pandey, A. Abusleme, and A. Seabaugh, "Switching dynamics of ferroelectric Zr-doped HfO$_2$," *IEEE Electron Device Lett.*, vol. 39, no. 11, pp. 1780–1783, Nov. 2018.

[38] I. Urbanavičiūtė, T. D. Cornelissen, X. Meng, R. P. Sijbesma, and M. Kemerink, "Physical reality of the Preisach model for organic ferroelectrics," *Nature Commun.*, vol. 9, no. 1, pp. 1–11, Dec. 2018.

[39] Z. Liu, H. Jiang, B. Ordway, and T. P. Ma, "Unveiling the apparent 'negative capacitance' effects resulting from pulse measurements of ferroelectric-dielectric bilayer capacitors," *IEEE Electron Device Lett.*, vol. 41, no. 10, pp. 1492–1495, Oct. 2020.

[40] Y. Xiang *et al.*, "Physical insights on steep slope FeFETs including nucleation-propagation and charge trapping," in *IEDM Tech. Dig.*, Dec. 2019, pp. 21.6.1–21.6.4.

[41] M. N. K. Alam *et al.*, "HfZrO ferroelectric characterization and parameterization of response to arbitrary excitation waveform," in *Proc. IEEE SOI-3D-Subthreshold Microelectron. Technol. Unified Conf. (S3S)*, Oct. 2019, pp. 1–3.

[42] A. K. Saha, K. Ni, S. Dutta, S. Datta, and S. Gupta, "Phase field modeling of domain dynamics and polarization accumulation in ferroelectric HZO," *Appl. Phys. Lett.*, vol. 114, no. 20, May 2019, Art. no. 202903.